Increasing Resolution in Exploration Biostratigraphy – Part 1

F.M.Gradstein (1), A.Bowman (2), A.Lugowski (3) and O.Hammer (1)

(1) Geological Museum, University of Oslo, N-O318 Oslo, Norway
(2) Chevron Energy Technology Co, 14141 SW Freeway, Sugarland, TX 77478, USA
(3) Purdue University, West Lafayette, IN 47907, USA.

Dedication

This study is dedicated to the memory of our friend and colleague Garry Jones, a staunch supporter of quantitative stratigraphic methods in exploration micropaleontology.

Abstract

Crossplots with Ranking & Scaling (RASC) and Constrained Optimization (CONOP) zonal sequences increase stratigraphic resolution and correlation potential of biozonations. The crossplots reveal which events do and which do not not deviate their stratigraphic position from well to well, and how well they track their average stratigraphic level. The methodology solves the problem that conventional fossil zonations do not rank taxa according to the degree of diachroneity of range endpoints in a correlation scheme. Part 1 of this study deals with North Sea biostratigraphic data, and part 2 with a dataset from the Gulf of Mexico.

Introduction

This study outlines a simple method to rank the stratigraphic fidelity of fossil events using zonal crossplots of RASC (Ranking & Scaling) and CONOP (Constrained Optimization). A paleontological event is the presence of a taxon in its time context, derived from its position in a sediment sequence. For stratigraphic purposes we recognize and apply first, first common or consistent, acme, last common or consist and last occurrence events. High fidelity of such events means they do not deviate much their stratigraphic position from well to well, and track their average stratigraphic level well. To understand the new approach, we have to understand how RASC and CONOP results differ, and how they can be similar.

The methods yield the following results (Gradstein et al., 1985; Sadler, 2001):

A. (RASC) Most likely optimum sequence of events; this is an ordinal composite standard, where calculated event positions in the composite are averages of all (well) section positions encountered. The

composite standard levels show estimates of event variance.

B. (RASC) Scaling of the optimum sequence; this is a composite standard with interval zones.

C. (CONOP) Composite standards with display of penalty (misfit) of events, according to two strategies:

1) event positions in the composite are unconstrained, and can move either up or down, not unlike RASC
2) event positions in the composite are maximized, either stratigraphically upwards (for tops) or downwards (for bases), as in conventional graphic correlation seeking total stratigraphic ranges. Using this strategy, events from the lower part of ranges generally move downwards in the composite standard, and events in the upper part of ranges upwards.

Figure 1 graphically illustrates different run strategies using first (lowest) and last (highest) occurrence events of a taxon in eight (well) sections taxa. RASC finds the average first and average last occurrence of an event, and hence constructs an average range; the range endpoints have an uncertainty attached, hence the RASC method is probabilistic. CONOP can be instructed to model either average ranges (unconstrained moves mode) or total ranges (maximizing moves mode); CONOP both mimicks probabilistic methods and models deterministic stratigraphic solutions. For both methods to work well, datasets should hold the stratigraphic occurrences of a reasonable number of taxa (e.g. 50 or more) in 10 or more sections.

Both RASC and CONOP also have a provision in their program runs that event positions are not allowed to move, and are correlated as locally observed. An example of an event that may not be allowed to move (relative to its neighbours) is a distinctive ash layer or log horizon.

Now we can create stratigraphic cross plots of the probabilistic RASC results (A or B option) with either the probabilistic (option 1) or deterministic (option 2) results using CONOP. If the events in a data set do not deviate much their relative position from well to well a correlation of the RASC optimum sequence results with the optimum sequence results using CONOP in strategy 1 will show limited or no cross-over of correlation lines. A two way scattergram of the results results in a tight-fitted channel. This approach was also explored by Cooper et al. (2001) for CONOP and RASC results in the Neogene of the Taranaki Basin, New Zealand. The authors calculated high correlation coefficients.

The opposite is true for events in a dataset that deviate their relative stratigraphic positions much from section to section. In this case the average and total stratigraphic ranges differ a lot, and this is readily modelled using

CONOP in option 2 mode versus RASC mode. Correlation of RASC and CONOP results will show more misfit, and two way graphs more scatter. The events that misfit more often have above normal variance, and are least useful for tracking their stratigraphic level.

Thus, the crossplot strategy enables well-site paleontologists to predict with confidence what the chances are a particular horizon has been identified, using best marker criteria. Since the methods target all data, not a regional ‘mindset’, correlation potential of wells is optimized.

Results

To test its utility, the crossplot method was applied to two datasets. One well-known datasets is from the North Sea (Gradstein & Bäckström, 1996; Kaminski & Gradstein, 2005) using Last Occurrence (LO) and Last Consistent Occurrence (LCO) events of dinoflagellates and foraminifers. The dataset comes from 30 wells and consists of 1430 occurrences of 88 taxa, and is reported in Part I of this study.

The second dataset, one that Garry Jones helped develop, is from the deep Gulf of Mexico, using LO, LCO, Acme, First Common Occurrence (FCO) and First Occurrence (FO) events of Neogene nannofossils and foraminifers. The Neogene zonation uses 1688 records of 85 events in 13 wells. Both datasets and the cross-plots are outlined below. This dataset is reported in part II of this study.

North Sea Geology: The North Sea region contain remnants of stratigraphically superimposed sedimentary basins of Late Paleozoic through Cenozoic age, like stacks of incomplete pancackes. The regional history is complex; differential subsidence and repeated uplifts are related to extensive mobilisation of the North Atlantic rift systems. Widespread sealevel rise took place in mid to late Cretaceous time, creating extensive transgression. A Late Cretaceous through Danian chalk blanket formed, originally also covering much of Great Britain and extending across the North Sea, Holland, northern Germany, and Denmark; this "chalk sea" was 200-400 m deep in places. In the northern part of the North Sea, west of Shetlands and offshore Norway, coeval marine deposition was of a fine-grained terrigenous nature, with marls and shales rather than carbonates.

Deeper water, bathyal sediments, including minor and major gravity flow, siliciclastic wedges, of middle to Late Cretaceous, and of Paleogene age are widespread and contain diversified agglutinated benthic

assemblages. In the southern part of the central North Sea, where deep water conditions prevailed into the Miocene, the agglutinated assemblage accordingly extends stratigraphically upwards.

Most diversified, most abundant, and most widespread agglutinated assemblages are found in the fine-grained, deep marine shales that were laid down during the rapid subsidence of the basins in the late Paleocene (Jones, 1988; Gradstein & Bäckström, 1996). This was the time when Paleogene seafloor spreading started in the Atlantic Ocean, north of the Charlie Gibbs fracture zone.

The large scale deposition of volcanic tuffs (Balder Fm) during the earliest Eocene coincides with the eruption of major flood basalts in eastern Greenland and Rockall, at the onset of seafloor spreading in the Norwegian Sea. The ash deposit is a prominent North Sea seismic reflector. Due to the flood-basalt outpourings, the North Sea became restricted, as reflected in the widespread distribution of diatoms, including the now pyritized pillbox *Fenestrella antiqua*, and virtual absence of bottom fauna in the severely dysaerobic basin. Surface water salinity may have been below normal.

A major terrigenous clastic feature in the Central North Sea and West of Shetlands is the presence of large sand bodies intercalated in the upper Paleocene to lower Eocene, considered to be deltaic lobes, deeper water sheet sands and turbidites of late Paleocene to early Eocene age. These deep water sands form the producing horizons in the Forties, Montrose, Frigg, Lomond, Cod and many other oil and gas fields. Studies of the Forties Field Paleocene reservoirs show the presence of typical deep marine fan complexes, with prodeltaic shales and silts passing upward through fine sandstones of the prograding delta slope, which in turn are overlain by coarser sandstones deposited in distributary channels on the delta top.

During the Eocene regional subsidence slowed down, terrigenous clastic supply diminished, and by mid-Cenozoic time the northern North Sea, Viking Graben had filled, but in the more southern North Sea, Central Graben deep marine sedimentation lasted until the middle Miocene. Rapid, basin-wide middle Miocene through Pleistocene basinal subsidence and concommittant uplift of basin edges, led to massive late stage sediment fill deposited in shallow water depths. The cause of this neotectonic phase results may be intensification and re-orientation of compressional intra-plate stresses perpendicular to the basin axis, concommittant with the Alpine orogeny in southern and central Europe. Localised late Miocene sediment condensation was probably caused by the effects of rapid eustatic sealevel lowering in a widespread shallow-marine setting. During the Pleistocene the northern part of the North Sea experienced glacial deposition and erosion.

During the active Paleocene to Eocene phase of North Sea basin subsidence, benthic foraminiferal faunas were markedly different from Central Graben to onshore outcrops. The former were deposited in middle to upper bathyal water depths (< 1000 m), whereas onshore deposits were formed in neritic environments (< 200 m). Only in the late Paleogene (Oligocene) and Neogene phase of basinal infilling did benthic foraminiferal faunas become gradually more homogeneous over the entire area, although the central part of the North Sea Basin remained deep up to the middle Miocene, as shown by the persistence there of an agglutinated flysch-type fauna, and recurrent incursions of warm-water planktonic foraminifera. Correlations between the onshore and North Sea Basin succession in the Paleocene and Eocene (at least) is best achieved by dinoflagellate cyst biostratigraphy, integrated with the biostratigraphy provided by the calcareous plankton (foraminifera and nannoplankton) and benthic foraminifera, magnetostratigraphy and volcanic ash stratigraphy. This way a correlation network has been established over NW Europe, which serves as the background against which the probabilistic zonation was developed.

North Sea Biostratigraphy: A total of 30 wells in the Viking and Central Grabens of the North Sea were selected for the zonations, using RASC and CONOP.

The record used for RASC consists of 1360 occurrences of 100 taxa of benthic and planktonic foraminifera, dinoflagellates, miscellaneous microfossils and 6 log markers. Almost all events are last occurrences (LO) in relative time, with two Last Common Occurrences (LCO). Each event occurs in at least 5 out of 30 wells, leaving 107 events; 12 unique events (occurring in fewer than 5 wells) that are useful for age calibration were also inserted. Figure 2 shows the RASC optimum sequence with standard deviations ; the average standard deviation (solid line) is 1.56; 55 out of 92 events have a standard deviation below average; unique events have no variance calculated. Two taxa, *Reticulophragmoides jarvisi* and *Cystammina pauciloculata* show erratic LO event positions in the wells, resulting in high standard deviations and outlier penalty points; these taxa were deleted from the record.

In Figure 3 is the RASC scaled optimum sequence with zones assigned subjectively. There are 18 zones and subzones, named NSR 1 - 13 (North Sea Rasc), of early Paleocene through early Pleistocene age. Large breaks (at events 129, 50, 206, 6, 266 and 23) indicate transitions between natural microfossil sequences, and/or hiatusses. The zones contain 33 agglutinated benthic events (32x LO and 1x LCO events) for 32 taxa, 29 of which are described in detail in Kaminski & Gradstein (2005).

Relative to the zonation for offshore northeast Canada (Kaminski & Gradstein 2005, Figs 14 and 15) many more agglutinated foraminiferal taxa are included, in part because the record is more diverse, and in part because of more detailed sampling and more detailed taxonomy. Both late Paleocene and early Oligocene assemblages are markedly diverse, and totally or largely devoid of calcareous benthic and planktonic taxa. One reason for the greater diversity in the North Sea Paleogene record may be less competition from calcareous benthic taxa, relative to the (more fertile and less restricted ?) Canadian Atlantic margin.

The total stratigraphic range of taxa may extend younger than the average stratigraphic range, with the result that the average last occurrences displayed in the RASC zonation of Figures 2 and 3 may be slightly older. On average, event observation in the wells may be closer to the average stratigraphic position than the last occurrence end point of the taxa in a fossil ranges chart that depicts total ranges.

Average LO or LCO events of agglutinated taxa typical for the North Sea Paleogene are:

1. Zone NSR2, late Paleocene: *Ammoanita ingerlisae, A. ruthvenmurrayi, Reticulophragmium pauperum, R. garcilassoi, Spiroplectammina spectabilis* LCO, *Rzehakina minima, Placentammina placenta, Caudammina excelsa,* and *Cystammina sveni*; the latter two have relatively high standard deviations (Figure 2); *A. ingerlisae, A. ruthvenmurrayi,* together with rare *Conotrochammina voeringensis* are confined to the lower part of the zone
2. Zone NSR4, early Eocene: *Recurvoidella lamella* and *Spiroplectammina navarroana*. The zone is named after the easily recognisable planktonic *Subbotina patagonica,* which has a circum Atlantic productivity event in the middle part of the early Eocene (see Gradstein *et al*., 1994, p. 37), when pink marls occur.
3. Zone NSR5, early Middle Eocene: *Spiroplectammina spectabilis* LO, *Ammomarginulina aubertae*, and *Haplophragmoides kirki*; the degree of uncertainty for the LO events of the three taxa is fairly high.
4. Zone NSR6A, late Middle Eocene: *Reticulophragmoides amplectens*, and *Ammosphaeroidina pseudopauciloculata*; the latter event has a fairly high standard deviation; it may be found as young as early Oligocene.
5. Zone NSR7A, early Oligocene: *Annectina biedai, Haplophragmoides walteri, Karreriella seigliei*, and particularly *Adercotryma agterbergi*. The LO events of *H. walteri* and *A. biedai* are often older, and have high standard deviations.

6. Zone NSR7B, early Oligocene: *Ammodiscus latus* and *Reticulophragmium rotundidorsatum*, both with fairly high standard deviations. The cosmopolitan calcareous benthic *Turrilina alsatica* is characteristic for this zone.
7. Zone NSR8, late Oligocene: *Spirosigmoilinella compressa*; rare specimens may be found younger

Compared to the RASC zonation, the North Sea optimum sequence using CONOP is not much different. The data set and optimum sequence stack (Table 2) is virtually the same as used with RASC. CONOP was executed in the unconstrained (BOB) mode, event positions in the composite are unconstrained, and can move either up or down, not unlike RASC

Figure 3 is a crossplot of the RASC and CONOP (BOB mode) optimum sequences. Spearman's rank correlation is 0.99595 and Kendall' tau 0.95612. One may argue that *G.subglobosa* var., *G.venezuelana* and maybe also *G.trilobus* and *W.symmetrica* are stacked too old with Conop and /or too young with RASC. The first two have high variances; the last one only occurs in 3 wells.

Figure 4 is the same plot, but here CONOP event last occurrences are maximized (socalled DISappearance mode), resulting in looser fit to the RASC optimum sequence, although Spearman's rank correlation is still a high 0.98966 and Kendall's tau 0.92671. Subjectively, several stratigraphically conclusions may be drawn. The average last occurrences of *B.frigida, M.cylindrica, E.elegans, R.rotundidorsata, C.sveni, C.excelsa,* and Calc. benthics spp. locally differ much from the uppermost ranges, as found in some wells (RASC has tables showing in which wells), and RASC variances are also high. The *R.rotundidorsatum* extension is part of a trend with stratigraphically nearby *C.cancellata, C.placenta*, Coarse agglutinated spp., *G.girardana,* Silicious biofacies and also *G. praebulloides* locally (Central Graben of the North Sea) extending one or even two zones younger. *C.dutemplei, C.subglobosa* var., *G.trilobus* (again) are either stacked too old in CONOP, or too young in RASC. North Sea Log marker G, Log F and Log E are stacked too old in CONOP, since their stratigraphic position in the RASC solution was independently confirmed (see Gradstein & Bäckström, 1996). In this particular CONOP run, the log markers were treated as marker (ASH) horizons, allowing minimal stratigraphic movement; this seems to result in underplotting relative to the DIS events.

Although many of the stratigraphic diachroneity conclusions drawn above also could be derived from RASC results alone, the bias is confidence in one method only. Deriving these conclusions from two independent methods strengthens the stratigraphic insight and geologic utility of the data.

Illustrations

Table 1

North Sea exploration wells studied for foraminifers, dinoflagellates, miscellaneous microfossils and log markers.

Figure 1. Graphic illustration of the manner (lowest) and last (highest) occurrence events of a taxon in eight (well) sections are treated by respectively Ranking & Scaling (RASC), and by Constrained Optimization (CONOP). RASC finds the average first and average last occurrence of events, and hence constructs an average range; the range endpoints may have an uncertainty attached; the method is probabilistic. CONOP can be instructed to model either average ranges or total ranges.

Figure 2

North Sea Cenozoic Optimum Sequence with standard deviations, calculated with the RASC (Ranking & Scaling) program. The record consists of 1360 occurrences of 100 taxa of benthic and planktonic foraminifera, dinoflagellates, miscellaneous microfossils and 6 log markers in 30 wells. Almost all events are last occurrences (LO) in relative time, with two Last Common Occurrences (LCO). Each event occurs in at least 5 out of 30 wells, leaving 107 events; 12 unique events (occurring in fewer than 5 wells) were also inserted. The average standard deviation (solid line) is 1.56; 55 out of 92 events have a standard deviation below average; unique events have no variance calculated.

Figure 3

North Sea Scaled Cenozoic Optimum Sequence, calculated with the RASC (Ranking & Scaling) program. The scale is relative, and is derived from the cross-over frequency of all optimum sequence events. Eighteen NSR (North Sea RASC) zones are recognised of Paleocene through Plio-Pleistocene age (Gradstein & Bäckström, 1996). Large scaling breaks (at events 129, 50, 206, 6, 266 and 23) indicate transitions between natural microfossil sequences, the result of hiatuses and /or lithological and facies changes. The zones contain 33 agglutinated benthic foraminiferal events (32x LO and 1x LCO events) for 32 taxa, 29 of which are described in Kaminski & Gradstein (2005).

Figure 4

Crossplot of the Ranking & Scaling (RASC) and Constrained Optimisation (CONOP, BOB mode) optimum sequences. The (stratigraphic) fit is very good. Spearman's rank correlation is 0.99595 and Kendall' tau 0.95612. One may argue that *G.subglobosa* var., *G.venezuelana* and maybe also *G.trilobus* and *W.symmetrica* are stacked too old with CONOP and /or too young with RASC. The first two taxa have high variances; the last one only occurs in 3 wells.

Figure 5

Same plot as in Figure 4, but now CONOP event last occurrences are maximized (socalled DISappearance mode), resulting in looser fit to the RASC optimum sequence, although Spearman's rank correlation is still a high 0.98966 and Kendall's tau 0.92671. For details see text.

References

Cooper, R.A., Crampton, J.S., Raine, I., Gradstein, F.M., Morgans, H.E.G., Sadler, P.M., Strong, C.P., Waghorn, D., and Wilson, G.J., 2001. Quantitative biostratigraphy of the Taranaki Basin, New Zealand: A deterministic and probabilistic approach. American Association of Petroleum Geology Bulletin 85 (8), pp. 1469-1498.

Gradstein, F.M., Agterberg, F.P., Brower, J.C. and Schwarzacher, W. 1985. Quantitative Stratigraphy. Reidel Publishing Company, Dordrecht and Unesco, Paris, 598 pp.

Sadler, P., 2001. Constrained optimization approaches to the paleobiological correlation and seriation problems. A user guide and reference manual to the CONOP program family. Unpublished, author released document.

Gradstein, Felix & Bäckström, Sven, 1996. Cainozoic biostratigraphy and palaeobathymetry, northern North Sea and Haltenbanken. Norsk Geologisk Tidskrift 76, pp. 3-32.

Kaminski, M.A. and Gradstein, F.M., 2005. Atlas of Paleogene Cosmopolitan Deep-water Agglutinated Foraminifera. Grzybowski Foundation, Special Publication 10, 548 pp.

Increasing Resolution in Exploration Biostratigraphy – Part II

A.Bowman (1) and F.M.Gradstein (2), A.Lugowski (3) and O.Hammer (2)

(1) Chevron Energy Technology Co, 14141 SW Freeway, Sugarland, TX 77478, USA
(2) Geological Museum, University of Oslo, N-O318 Oslo, Norway
(3) Purdue University, West Lafayette, IN 47907, USA.

Introduction

Exploration biostratigraphy in the oil and gas industry typically focusses on extinction levels ("tops") of species observed in a sedimentary sequence. Increased biostratigraphic resolution is gained through the investigation of the potential usefulness of other and non-traditional bioevents (first downhole increases, acmes, etc.). The greater the biostratigraphic resolution, the more traceable horizons are created, which allow professional geoscientists to better understand the subsurface geology. Crossplots with Ranking & Scaling (RASC) and Constrained Optimization (CONOP) zonal sequences increase stratigraphic resolution and correlation potential of biozonations. The new method will be demonstrated in the deep Gulf of Mexico, using Neogene petroleum exploration data.

Gulf of Mexico

The Gulf of Mexico (GOM) has a rich tradition of petroleum exploration. Many wells have been drilled, producing an extensive micropaleontological database, mostly consisting of calcareous nannofossils and foraminifers (benthic and planktonic).

The Mad Dog Field occupies Blocks 782, 783, and 826 in the Green Canyon protraction area of the deepwater Gulf of Mexico, approximately 200 miles south of New Orleans (Figure 1). The average water depth of the field area is between 4500 and 6800 feet. The field itself is a faulted, four-way closure located under the Sigsbee escarpment. Three reservoir sands have been discovered in the lower Miocene, and were termed the DD, EE, and FF. The sands have been interpreted as turbidite sands, and are laterally continuous over several miles. The DD, EE, and FF sands are medium to fine grained, and have about 360 feet of total thickness (Smith *et al*., 2001). The field was first discovered in 1998, and is currently in the production phase. Production began in January 2005, and total reserves are estimated at 200-450 million barrels oil equivalent.

With the reservoir sands located under salt, and at subsurface depths greater than 20,000 feet, seismic correlation and mapping are difficult. Thus, biostratigraphic data are an essential tool for correlating key sands.

Methods

Thirteen wells that collectively spanned the GOM deepwater Miocene section were chosen for the study. Wells were chosen based on the quality of biostratigraphic data, and depth of penetration within the Miocene. The key focus was to incorporate as many wells as possible in order to fully represent the proper order of events in the Miocene GOM.

In an effort to increase success with correlations among wells in the Mad Dog Field, the Ranking and Scaling (RASC) and Constrained Optimization (CONOP) methods were applied to arrive at a high-resolution biozonation using as many data as possible. The methods for creating the optimum sequence are outlined in Gradstein *et al*. (this volume); here we focus on data preparation for the Mad Dog program runs.

The initial process required evaluating and validating bioevents of hundreds of Miocene age taxa using hard copy range charts (BugCad plots), followed by analysis of the documented bioevents through the biostratigraphic software program Integrated PaleoSystem (IPS). This two stages process yielded the placement of the more common types of bioevents (species range tops and bases), as well as discerning new and useful subordinate bioevents. The RASC result was an optimum stratigraphic order of bioevents, with uncertainty of the reliability of each.

Defining Bioevents:

For RASC analysis to be of use, it is crucial to input quality data. Therefore producing and following "rules" is necessary when documenting various bioevents. Determining the criteria that defines each bioevent is an important step. Uncertainty exists when correlating non-traditional bioevents among wells because biostratigraphers may have different ideas as to how non-traditional bioevents are defined. The rules produced for this study were created based on careful examination of the data, and were modified if they were too complex or illogical. The final set of eight taxonomic-stratigraphic rules were strictly followed during the process of documenting bioevents for the deepwater GOM Miocene wells (Table 1).

Capturing and Recording Bioevents:

Bioevents were captured for calcareous nannofossil and foraminifera species using the BugCad distribution charts and IPS software. A key asset of IPS is the ability to calculate and plot peaks in species abundance and species diversity within a well, therefore making it possible to choose the key bioevents in condensed intervals associated with periods of maximum flooding (within fine-grained lithologies with the best preservation).

Each well had between 32 and 57 bioevents, with the average number of bioevents per well being 46. The number of bioevents in each well is a function of depth of penetration (age), and quality of microfossil preservation. Data from each well was then recorded in ASCII files, listing depth for each specific bioevent and the name of the particular bioevent (ex. "Sphenolithus dissimilis TOP"). Recorded bioevents were then prepared for several iterations of RASC.

RASC and CONOP Analysis

During RASC runs, the statistical requirements were altered as necessary in order to achieve the most useful output. The main statistical parameter to alter during iterations is the "k value," or the minimum number of wells that a bioevent must occur in. This threshold directly controls the stratigraphic results. As the "k value" increases, the total number of bioevents in the optimum sequence decreases. The opposite is obviously true if the "k value" is decreased.

RASC analysis was carried out using threshold k values of 7 and of 6. The "k=7" RASC run produced 71 total bioevents in the optimum sequence, 49 of which had standard deviations below the average of 4.70. The "k=6" RASC run left 91 bioevents in the optimum sequence, with 61 bioevents possessing standard deviations lower than the average (avg. = 4.80).

The same data were also analyzed with the Constrained Optimisation (CONOP) method. CONOP in average event 'ranges' (BOB) mode yielded results closely comparable to RASC, with a more diverging sequence using the DIS mode that maximizes event range endpoints

Figure 2 is a crossplot of the RASC and CONOP (BOB mode) that shows good coherence and low scatter, whereas the crossplot of Figure 3 with CONOP in DIS mode produced considerable scatter. Outlier events in the upper left quadrant of Figure 3 are events that vary their BASE or LO much from well to well; outlier events in the lower right quadrant are events that vary their FDI, HO or TOP occurrence much from well to well. Seventeen of these outliers were thus deleted from further RASC runs.

Since a threshold k value equal to 6 produces the most bioevents with minimal change in data quality, and results in the most useful optimum sequence, analysis was continued with this run. Firstly, bioevents that had standard deviations greater than the average were omitted from the final optimum sequence. Next, all bioevents involving the highest occurrence (HO) and lowest occurrence (LO) of species were deleted from the RASC optimum sequence, as they generally created confusion when related to the true extinction top and true evolutionary base of the various species. This step was performed based on knowledge and experience of calcareous nannofossil biostratigraphy.

After the less reliable bioevents were thus omitted, a total of 38 bioevents were retained, of which 34 were calcareous nannofossil events and 4 were foraminifer events. Table 2 lists the final, curtailed optimum sequence, showing the bioevents with standard deviation, and the number of wells in which each occurred.

In an effort to apply the final biozonation created by the optimum sequence, four wells within the Mad Dog field were used in this study to refine the biostratigraphic correlation. The names of the wells have been omitted for proprietary concerns. The purple correlation lines are bioevents used from the optimum sequence. Most bioevents throughout the entire Miocene have very low crossover frequencies. However, because the most crucial reservoirs in the Mad Dog Field are Middle and Early Miocene age, the focus of the biostratigraphic correlations was directed to these intervals.

Figure 4 illustrates the biostratigraphic correlations for the entire Miocene, created using the bioevents produced from the optimum sequence. Figure 5 shows an enlarged portion of the correlation for the Lower to Middle Miocene sedimentary section. The standard and commonly used bioevents (with associated standard deviations), along with the reliable seismic reflector (MMR) are:

Discoaster pentaradiatus BASE (S.D. = 3.19)
Discoaster bollii TOP (S.D. = 1.89)
Minylitha convalis BASE (S.D. = 2.63)
Discoaster bollii BASE (S.D. = 2.33)
Discoaster prepentaradiatus BASE (S.D. = 2.26)
Catinaster coalitus TOP (S.D. = 1.89)
Discoaster exilis TOP (S.D. = 1.73)
Coccolithus miopelagicus TOP (S.D. = 3.1)
Discoaster sanmiguelensis TOP (S.D. = 3.24)
Calcidiscus premacintyrei TOP (S.D. = 2.39)
MMR (Middle Miocene Reflector) (S.D. = 2.95)
Discoaster petaliformis TOP (S.D. = 1.97)
Sphenolithus heteromorphus BASE (S.D. = 3.24)

The most useful non-traditional bioevents produced from this work, and used for correlation of wells in the Mad Dog field include: *Sphenolithus heteromorphus* FDI, *Discoaster deflandrei* FDI, and *Discoaster petaliformis* FDI. The bioevents with lowest standard deviations and the associated Miocene NN Zone (Martini, 1971) are listed below:

NN10: *Discoaster quinqueramus* BASE (S.D. = 2.19)

NN6: *Cyclicargolithus floridanus* TOP (S.D. = 1.74)

NN5: *Sphenolithus heteromorphus* TOP (S.D. = 2.62)

NN3: *Sphenolithus belemnos* TOP (S.D. = 2.17)

NN2: *Triquetrorhabdulus carinatus* TOP (S.D. = 2.27)

Conclusions:

Biostratigraphic correlations between wells across fields are a crucial tool for mapping key sands. Increasing the biostratigraphic resolution also increases the success in understanding the connectivity and character of important stratigraphic units. The goal of this work was to determine new and reliable bioevents to help build a higher resolution biostratigraphic correlation throughout the Mad Dog Field. The steps followed to achieve this goal were: build criteria (rules) for establishing new bioevents to add biostratigraphic resolution, identify these new bioevents, run the new bioevents through RASC analysis to produce a valid optimum sequence, and use the produced optimum sequence for correlation of key sands in the Middle and Early Miocene intervals within the Mad Dog Field.

Results show the bioevents incorporated from the optimum sequence have low crossover frequencies, therefore allowing for a reliable high resolution biostratigraphic correlation in the Mad Dog Field. This work has provided proven value within the exploration and development realms, and has great potential as a valuable tool not only in the Gulf of Mexico, but worldwide as well.

Illustrations

Table 1
Eight different rules for stratigraphic bioevents were captured for calcareous nannofossils and foraminifers in the thirteen Miocene Gulf of Mexico wells studied.

Table 2
Miocene optimum sequence using Ranking and Scaling (RASC) on 13 wells in the Gulf of Mexico. The RASC run using events that occur in 6 or more wells (k=6) left 91 bioevents in the optimum sequence, with 61 bioevents possessing standard deviations lower than the average (avg. = 4.80). Bioevents involving the highest occurrence (HO) and lowest occurrence (LO) of species were deleted from the optimum sequence, as they generally created confusion when related to the true extinction top and true evolutionary base of the various species. This step was performed based on knowledge and experience of calcareous nannofossil biostratigraphy. After less reliable bioevents were omitted, a total of 38 bioevents were retained, of which 34 were calcareous nannofossil events and 4 were foraminifer events. The list shows the final Miocene

optimum sequence of bioevents with their standard deviations, and the number of wells in which each occurred. Foraminifera events are represented by a numeric sign (#).

Figure 1
The Mad Dog Field occupies Blocks 782, 783, and 826 in the Green Canyon protraction area of the deepwater Gulf of Mexico, approximately 200 miles south of New Orleans.

Figure 2
Crossplot of the RASC and CONOP (BOB mode) optimum sequences for the Miocene Gulf of Mexico. The (stratigraphic) fit is very good, the result of close convergence on the same optimum sequence using both methods.

Figure 3
The same crossplot as in Figure 2, but now CONOP event last occurrences are maximized (socalled DISappearance mode), resulting in a much looser fit to the RASC optimum sequence. Outlier events in the upper left quadrant are events that vary their BASE or LO much from well to well;outlier events in the lower right quadrant are events that vary their FDI, HO or TOP occurrence much from well to well. Seventeen of these outliers were thus deleted from further RASC runs.

Figure 4
Application of non-traditional bioevents from optimum sequence used in correlation of Mad Dog Field.

Figure 5
Zoomed in portion of well correlation for Mad Dog Field. Traditional and non-traditional bioevents from optimum sequence used to improve biostratigraphic correlations.

References

Gradstein, F.M., Bowman, A., Lugowski, A. and Hammer, O. (2008). Increasing Resolution in Exploration biostratigraphy-Part I. Computers and Geosciences, this volume.

Martini, E., 1971. Standard Tertiary and Quaternary calcareous nannoplankton zonation. In: Farinacci, A. (Ed.), Proceedings of the Second Planktonic Conference, Roma 1970: Roma, Tecnoscienza, pp. 739-785.

Smith, T., Kenney, D., DiMarco, M., Poulin, M., Trevena, A., Steffens, G., 2001. Geological and geophysical reservoir description at Mad Dog Field - An ultra-deepwater, sub-salt oil discovery in the Gulf of Mexico. In: Abstracts 2001 Unocal Technology Conference, Bangkok, Thailand, March 2001.

 1 Saga (N) 35/3-1
 2 Saga (N) 35/3-4
 3 Hydro (N) 34/8-1
 4 Saga 34/7-1
 5 Saga 34/7-2
 6 Saga 34/7-4
 7 Saga 34/7-15s
 8 Saga 34/7-22
 9 Saga 34/7-24s
10 Norsk Hydro 31/2-19S
11 Statoil 30/3-1
12 Statoil 30/3-A1
13 Total (UK) 3/25-1
14 Shell (UK) 9/23-1
15 Mobil (UK) 9/13-1
16 Mobil (UK) 9/13-3A
17 Mobil (UK) 9/13-5
18 Esso (N) 16/1-1
19 BP (UK) 15/20-2
20 Phillips (UK) 16/17-1
21 Phillips (UK) 16/29-2
22 BP (UK) 21/10-1
23 BP (UK) 21/10-4
24 Mobil (UK) 21/28-1
25 Shell (UK) 22/6-1
26 Phillips (UK) 23/22-1
27 Shell (UK) 29/3-1
28 Shell (UK) 30/19-1
29 Saga (N) 2/2-4
30 Amoco (N) 2/8-1

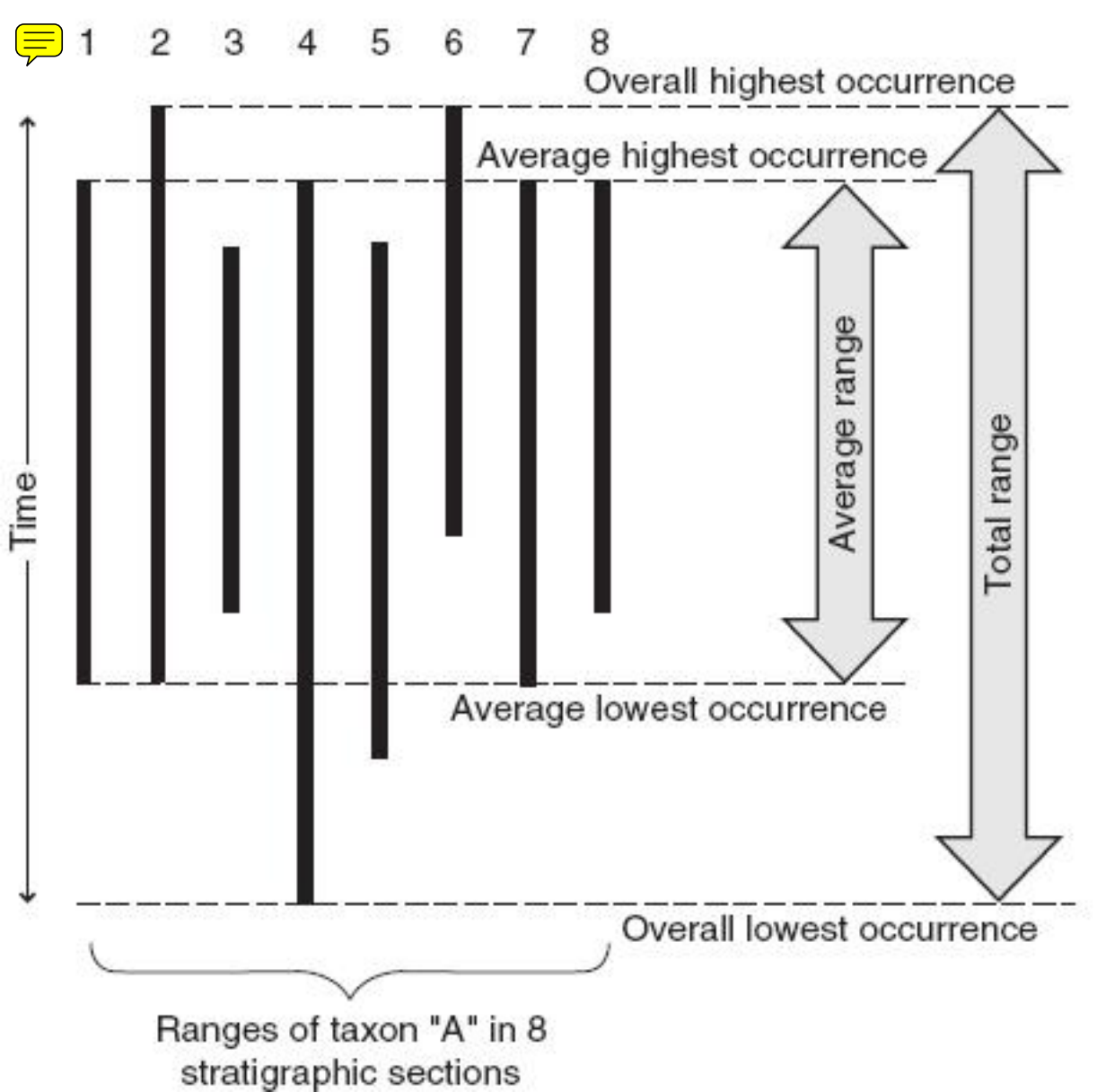
1
2
3
4
5
6
7
8
Overall highest occurrence
Average highest occurrence
Average range
Total range
Time
Average lowest occurrence
Overall lowest occurrence
Ranges of taxon "A" in 8 stratigraphic sections

Ranked Optimum Sequence of 107 Cenozoic Microfossil Events
30 wells North Sea; 1360 records; 5/3 run + 12 unique events

No.	&	UI			N	SD
1			240	Elphidium clavatum	5	0.633
2			77	Elphidium spp.	17	0.862
3			228	Cassidulina teretis	19	0.751
4			338	Bulimina marginata	7	0.849
5			1	Neogloboquadrina pachyderma	14	1.453
6			31	Cibicidoides scaldisensis	8	0.979
7			171	Buccella frigida	9	1.189
8	0	1	270	Cibicidoides grossa	16	0.846
9	-1	0	328	Ammonia beccarii	5	1.012
10			352	Nonion affine LCO	5	1.064
11			4	Globorotalia inflata	8	1.861
12			181	Cibicidoides dutemplei	6	1.806
13	0	1	316	Trifarina fluens	7	2.261
14	-1	1	159	Cibicidoides grossa LCO	6	1.642
15	-1	1	318	Monspeliensis pseudotepida	5	2.140
16	-1	0	23	Sigmoilopsis schlumbergeri	18	1.517
17			74	Neogloboquadrina humerosa	5	1.230
18			339	Globigerina bulloides	6	1.112
19	0	1	266	Globorotalia puncticulata	7	0.806
20	-1	0	269	Neogloboquadrina atlantica	13	1.053
21			5	**Globorotalia crassaformis		
22			411	Globocassidulina subglobosa var.	5	2.105
23			330	Cibicidoides pachyderma	6	2.007
24			130	Siphonina advena	6	1.031
25	0	1	6	Neogloboquadrina acostaensis	5	1.073
26	-3	0	81	Globoquadrina venezuelana	5	1.574
27			91	Diatoms/radiolarians LCO	13	1.253
28			301	**Bolboforma metzmacheri		
29			123	Globigerinoides trilobus	7	1.134
30			219	Martinotiella cylindrica	12	1.810
31			58	**Neogloboquadrina atlantica (dext)		
32			285	Caucasina elongata	8	1.376
33	0	1	125	Neogloboquadrina continuosa	6	2.257
34	-1	0	282	Uvigerina ex.gr. semiornata	6	1.257
35			207	NS Log G	11	1.459
36	0	1	236	G. ex.gr. praescitula zealandica	14	1.069
37	-1	0	334	Ehrenbergina variabilis	5	1.475
38			17	Asterigerina gurichi	19	1.422
39			18	Spiroplectammina carinata	6	2.751
40			71	Epistomina elegans	6	1.740
41			233	**Catapsydrax unicavus		
42			15	Globigerina praebulloides	15	2.155
43			3	**Deflandrea phosphoritica		
44			413	Silicious biofacies	9	0.923
45			351	Aulacodiscus insignis quadrata	5	1.311
46			20	Gyroidina girardana	11	1.911
47			128	**Distatodinium biffii		
48			24	Turrilina alsatica	13	2.519
49	0	1	176	Uvigerina gallowayi	5	0.730
50	-2	0	16	Ceratobulimina contraria	5	2.077
51	0	1	25	Coarse agglutinated spp.	28	2.049
52	-1	0	142	Gyroidina soldanii mamilligera	7	1.336
53			97	Cyclammina placenta	24	2.202
54			80	Cyclammina cancellata	5	1.644
55			182	Spirosigmoilinella compressa	21	1.194
56			259	Ammodiscus latus	9	1.724
57			41	**Wetzelliella symmetrica		
58			324	Aschemonella grandis	5	2.153
59			183	Reticulophragmium rotundidorsatum	12	1.932
60			140	Rotaliatina bulimoides	12	1.478
61			261	Haplophragmoides walteri	20	2.478
62			170	**Reticulophragmium acutidorsatum		
63			535	Annectina biedai	7	2.515
64			321	Dorothia seigliei	13	1.710
65			289	Adercotryma agterbergi	13	1.460
66			229	Recurvoides ex.gr. walteri	8	2.300
67			206	NS Log F	11	1.656
68	0	1	29	Reticulophragmium amplectens	24	1.223
69	-1	0	32	Ammosph.pseudopauciloculata	15	1.653
70			13	**Heteraulacacysta porosa		
71			12	Areosphaeridium diktyoplokus	7	1.947
72			192	**Karrerulina coniformis		
73			263	Ammomarginulina aubertae	16	1.214
74			260	Haplophragmoides kirki	15	1.608
75			68	Spiroplectammina spectabilis LO	24	1.412
76	0	1	117	Cenosphaera spp. LCO	10	1.466
77	-1	0	205	NS Log E	12	1.029
78			99	**Eatonicysta ursulae		
79			175	Reticulophragmium intermedium	5	1.299
80			86	Turrilina robertsi	5	2.317
81			279	Recurvoidella lamella	8	1.215
82			54	Spiroplectammina navarroana	19	2.227
83			50	Subbotina patagonica	15	1.242
84			22	Fenestrella antiqua	17	1.303
85			277	Tuff	7	0.787
86	0	1	28	Apectodinium augustum	6	1.135
87	-1	0	204	NS Log D	12	0.880
88			203	NS Log C	11	0.723
89			105	Rzehakina minima	7	0.649
90			76	Reticulophragmium pauperum	20	1.036
91			283	Reticulophragmium garcilassoi	8	1.225
92			284	Labrospira pacifica	7	1.763
93			310	Saccammina placenta	13	1.051
94			532	Cystammina sveni	13	1.798
95			57	Spiroplectammina spectabilis LCO	22	1.108
96			114	Alisocysta margarita	5	1.024
97			304	**Areoligera gippingensis		
98	0	1	129	Ammoanita ruthvenmurrayi	12	1.446
99	-1	0	134	Caudammina excelsa	12	1.806
100	0	1	353	Calcareous benthics spp.	5	2.074
101	-2	0	531	Ammoanita ingerlisae	5	2.116
102			61	Subbotina pseudobulloides	18	0.660
103			55	Gavelinella beccariiformis	15	0.842
104			60	Planorotalites compressus	14	0.741
105			107	Remesella varians	9	0.964
106			202	NS Log B	10	0.754
107			253	Subbotina triloculinoides	10	0.816

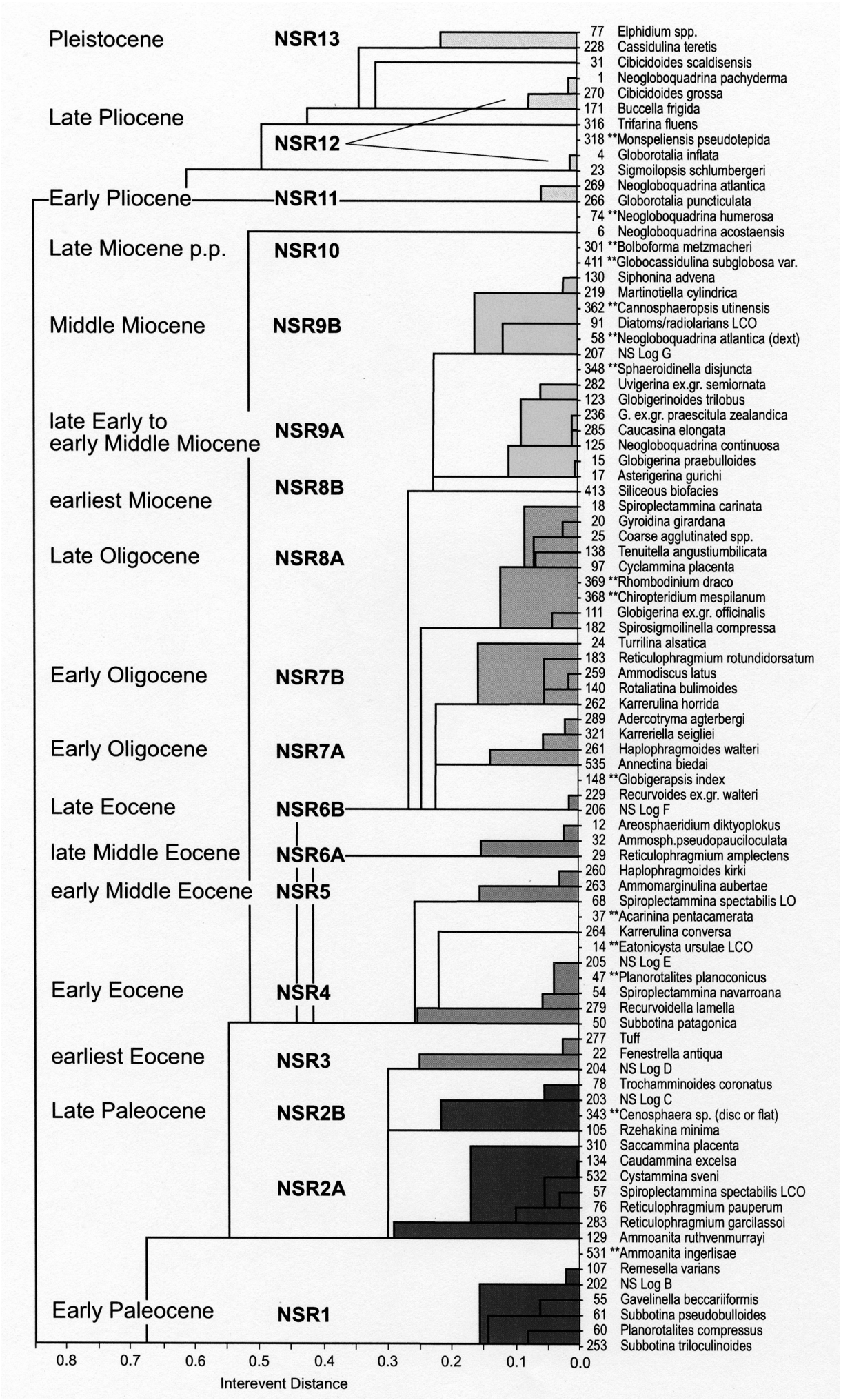
Pleistocene
NSR13
Late Pliocene
NSR12
Early Pliocene
NSR11
Late Miocene p.p.
NSR10
Middle Miocene
NSR9B
late Early to
early Middle Miocene
NSR9A
NSR8B
earliest Miocene
Late Oligocene
NSR8A
Early Oligocene
NSR7B
Early Oligocene
NSR7A
Late Eocene
NSR6B
late Middle Eocene
NSR6A
early Middle Eocene
NSR5
Early Eocene
NSR4
earliest Eocene
NSR3
Late Paleocene
NSR2B
NSR2A
Early Paleocene
NSR1
77 Elphidium spp.
228 Cassidulina teretis
31 Cibicidoides scaldisensis
1 Neogloboquadrina pachyderma
270 Cibicidoides grossa
171 Buccella frigida
316 Trifarina fluens
318 **Monspeliensis pseudotepida
4 Globorotalia inflata
23 Sigmoilopsis schlumbergeri
269 Neogloboquadrina atlantica
266 Globorotalia puncticulata
74 **Neogloboquadrina humerosa
6 Neogloboquadrina acostaensis
301 **Bolboforma metzmacheri
411 **Globocassidulina subglobosa var.
130 Siphonina advena
219 Martinotiella cylindrica
362 **Cannosphaeropsis utinensis
91 Diatoms/radiolarians LCO
58 **Neogloboquadrina atlantica (dext)
207 NS Log G
348 **Sphaeroidinella disjuncta
282 Uvigerina ex.gr. semiornata
123 Globigerinoides trilobus
236 G. ex.gr. praescitula zealandica
285 Caucasina elongata
125 Neogloboquadrina continuosa
15 Globigerina praebulloides
17 Asterigerina gurichi
413 Siliceous biofacies
18 Spiroplectammina carinata
20 Gyroidina girardana
25 Coarse agglutinated spp.
138 Tenuitella angustiumbilicata
97 Cyclammina placenta
369 **Rhombodinium draco
368 **Chiropteridium mespilanum
111 Globigerina ex.gr. officinalis
182 Spirosigmoilinella compressa
24 Turrilina alsatica
183 Reticulophragmium rotundidorsatum
259 Ammodiscus latus
140 Rotaliatina bulimoides
262 Karrerulina horrida
289 Adercotryma agterbergi
321 Karreriella seigliei
261 Haplophragmoides walteri
535 Annectina biedai
148 **Globigerapsis index
229 Recurvoides ex.gr. walteri
206 NS Log F
12 Areosphaeridium diktyoplokus
32 Ammosph.pseudopauciloculata
29 Reticulophragmium amplectens
260 Haplophragmoides kirki
263 Ammomarginulina aubertae
68 Spiroplectammina spectabilis LO
37 **Acarinina pentacamerata
264 Karrerulina conversa
14 **Eatonicysta ursulae LCO
205 NS Log E
47 **Planorotalites planoconicus
54 Spiroplectammina navarroana
279 Recurvoidella lamella
50 Subbotina patagonica
277 Tuff
22 Fenestrella antiqua
204 NS Log D
78 Trochamminoides coronatus
203 NS Log C
343 **Cenosphaera sp. (disc or flat)
105 Rzehakina minima
310 Saccammina placenta
134 Caudammina excelsa
532 Cystammina sveni
57 Spiroplectammina spectabilis LCO
76 Reticulophragmium pauperum
283 Reticulophragmium garcilassoi
129 Ammoanita ruthvenmurrayi
531 **Ammoanita ingerlisae
107 Remesella varians
202 NS Log B
55 Gavelinella beccariiformis
61 Subbotina pseudobulloides
60 Planorotalites compressus
253 Subbotina triloculinoides
0.8
0.7
0.6
0.5
0.4
0.3
0.2
0.1
0.0
Interevent Distance

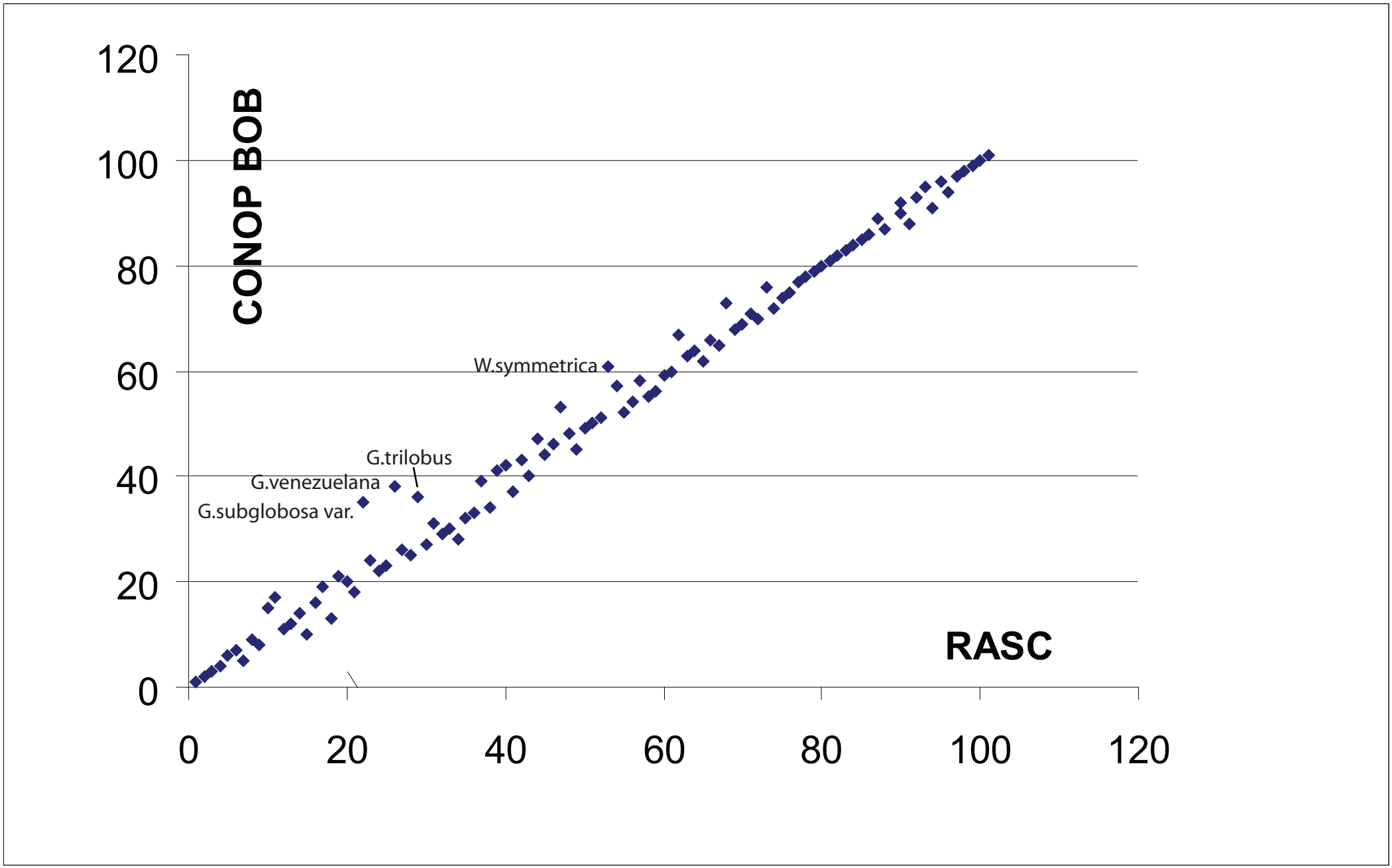
120
100
80
60
40
20
0
CONOP BOB
W.symmetrica
G.trilobus
G.venezuelana
G.subglobosa var.
RASC
0
20
40
60
80
100
120

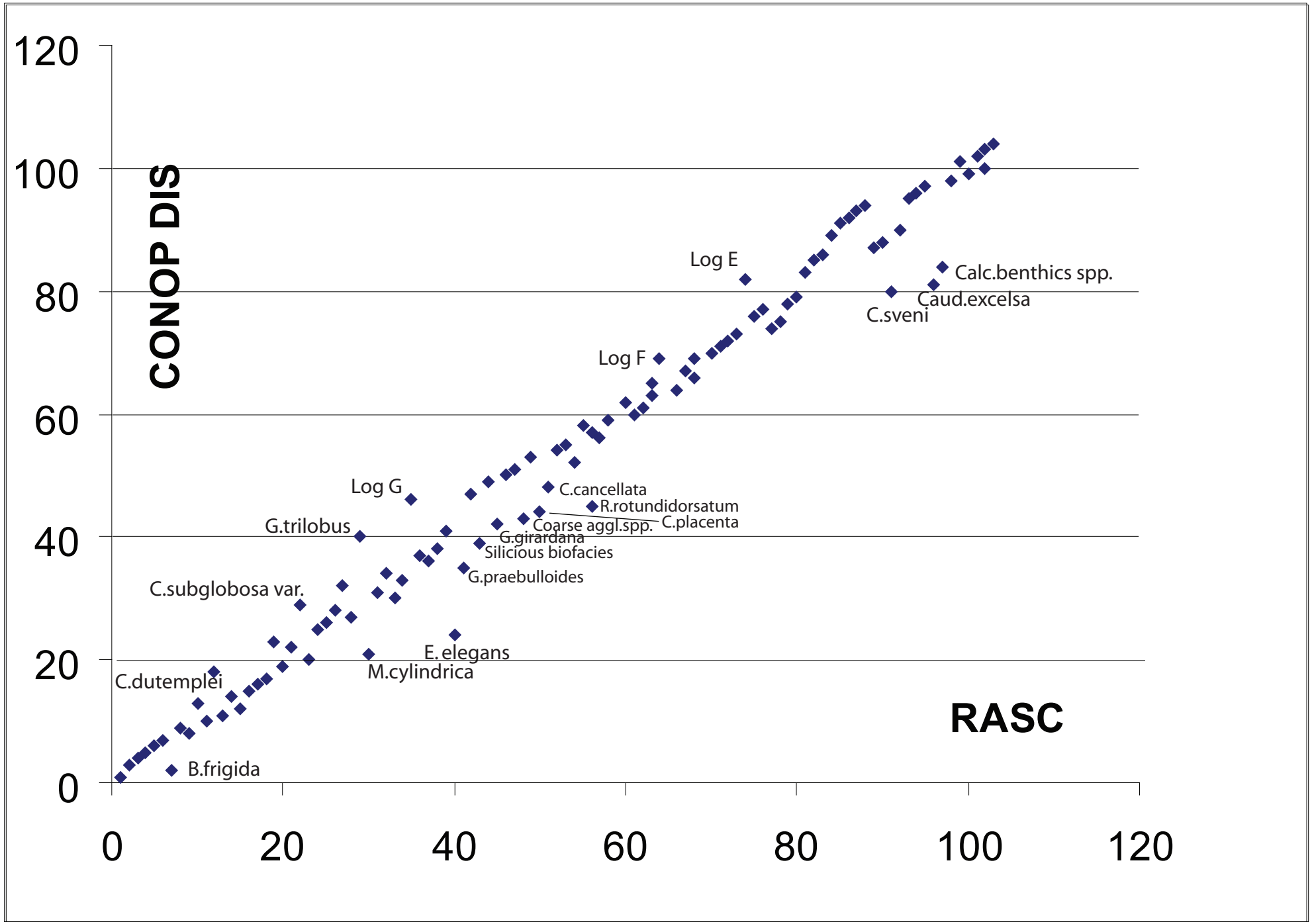
CONOP DIS
RASC
120
100
80
60
40
20
0
0
20
40
60
80
100
120
Log E
Calc.benthics spp.
Caud.excelsa
C.sveni
Log F
Log G
C.cancellata
R.rotundidorsatum
C.placenta
G.trilobus
Coarse aggl.spp.
G.girardana
Silicious biofacies
G.praebulloides
C.subglobosa var.
E. elegans
M.cylindrica
C.dutemplei
B.frigida

HO = **Highest stratigraphic occurrence**
cannot be in a sand body

TOP = Extinction level
Based on biostratigraphic interpretation

FDI = First downhole abundance increase
Change from low abundance (1, 2, 6 specimens) to at least 20

FDCO = First downhole common and consistent occurrence
"common" = 50 or greater
> 90 ft of "common" interval
no > 50s above FDCO event
no breaks > 90 ft in beginning of "common" interval (3 continuous occurrences)

LDCO = Last downhole common and consistent occurrence
Analogous to FDCO

ACME = Abundance spike
short and abrupt event; dramatic increase in abundance
if many possibilities, "best" ACME chosen

BASE = Evolutionary first appearance
Based on biostratigraphic interpretation

LO = Lowest stratigraphic occurrence
cannot be in a sand body

Event	S.D. (Avg. = 4.80)	Number of Wells
Discoaster pentaradiatus BASE	3.19	7
Discoaster surculus BASE	3.66	7
Discoaster quinqueramus BASE	2.19	6
Discoaster bollii TOP	1.89	6
Minylitha convallis BASE	2.63	7
Discoaster bollii BASE	2.33	10
Discoaster prepentaradiatus BASE	2.26	6
Discoaster neohamatus BASE	2.12	7
Discoaster brouweri BASE	4.20	7
Catinaster coalitus TOP	1.82	8
Discoaster exilis TOP	1.73	6
Coccolithus miopelagicus TOP	3.10	12
Discoaster musicus TOP	4.44	9
Discoaster sanmiguelensis TOP	3.24	10
Calcidiscus premacintyrei TOP	2.39	9
Globorotalia peripheroacuta TOP#	4.25	9
Cyclicargolithus floridanus TOP	1.74	11
Globorotalia peripheroronda TOP#	4.81	7
Discoaster deflandrei TOP	4.66	11
Sphenolithus heteromorphus TOP	2.62	11
MMR	2.95	8
Cyclicargolithus floridanus FDI	3.90	11
Sphenolithus heteromorphus FDI	2.75	11
Calcidiscus premacintyrei FDI	3.92	6
Discoaster petaliformis TOP	1.97	11
Globorotalia peripheroacuta BASE#	3.51	8
Orbulina universa BASE#	4.11	7
Discoaster petaliformis FDI	2.91	7
Helicosphaera ampliaperta TOP	3.69	10
Discoaster petaliformis BASE	4.09	9
Discoaster deflandrei FDI	1.93	8
Helicosphaera kamptneri-carteri ACME	4.50	9
Sphenolithus heteromorphus ACME	3.58	11
Sphenolithus heteromorphus BASE	3.24	7
Sphenolithus belemnos TOP	2.17	7
Discoaster calculosus TOP	3.63	8
Discoaster deflandrei ACME	4.20	6
Triquetrorhabdulus carinatus TOP	2.27	6

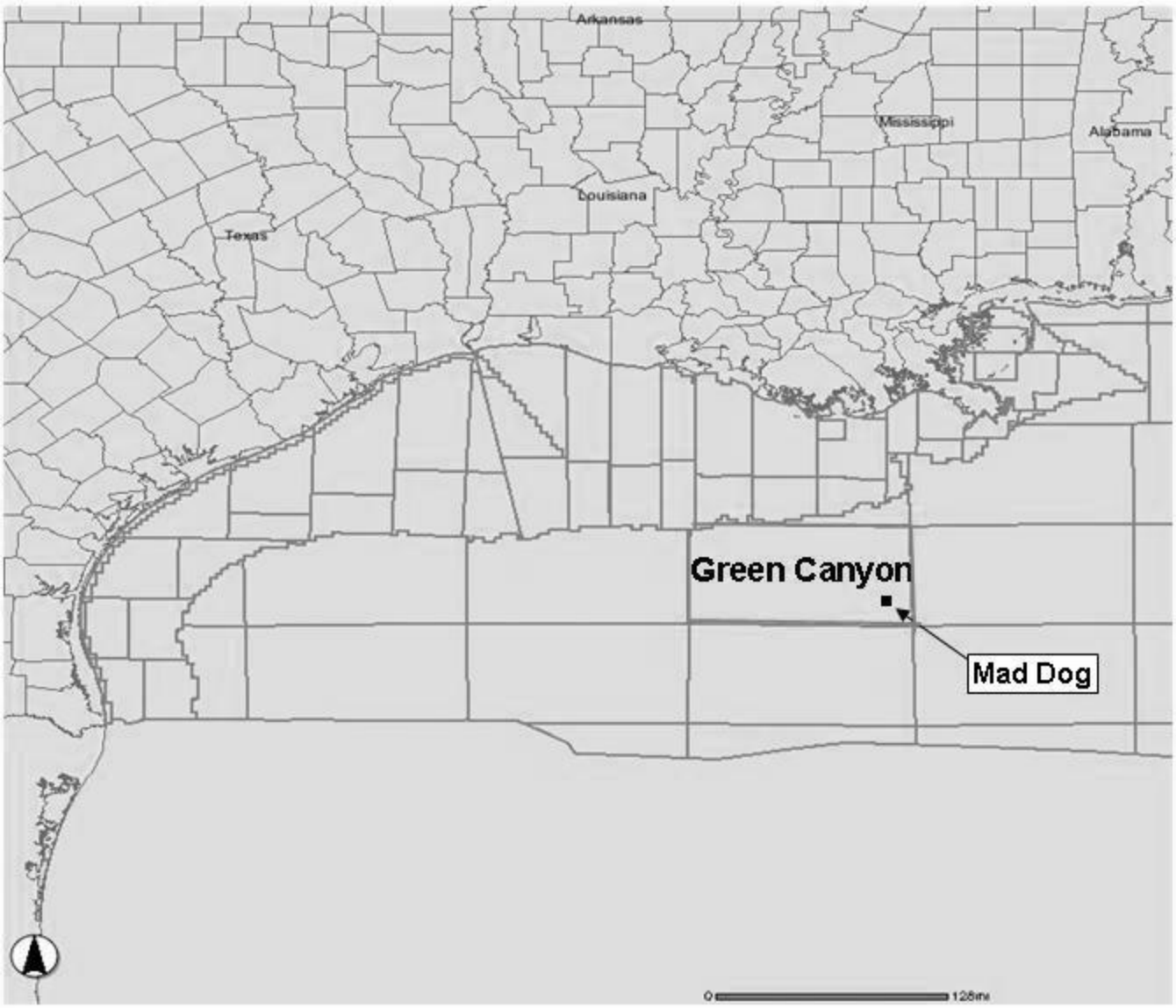

Green Canyon

Mad Dog Field

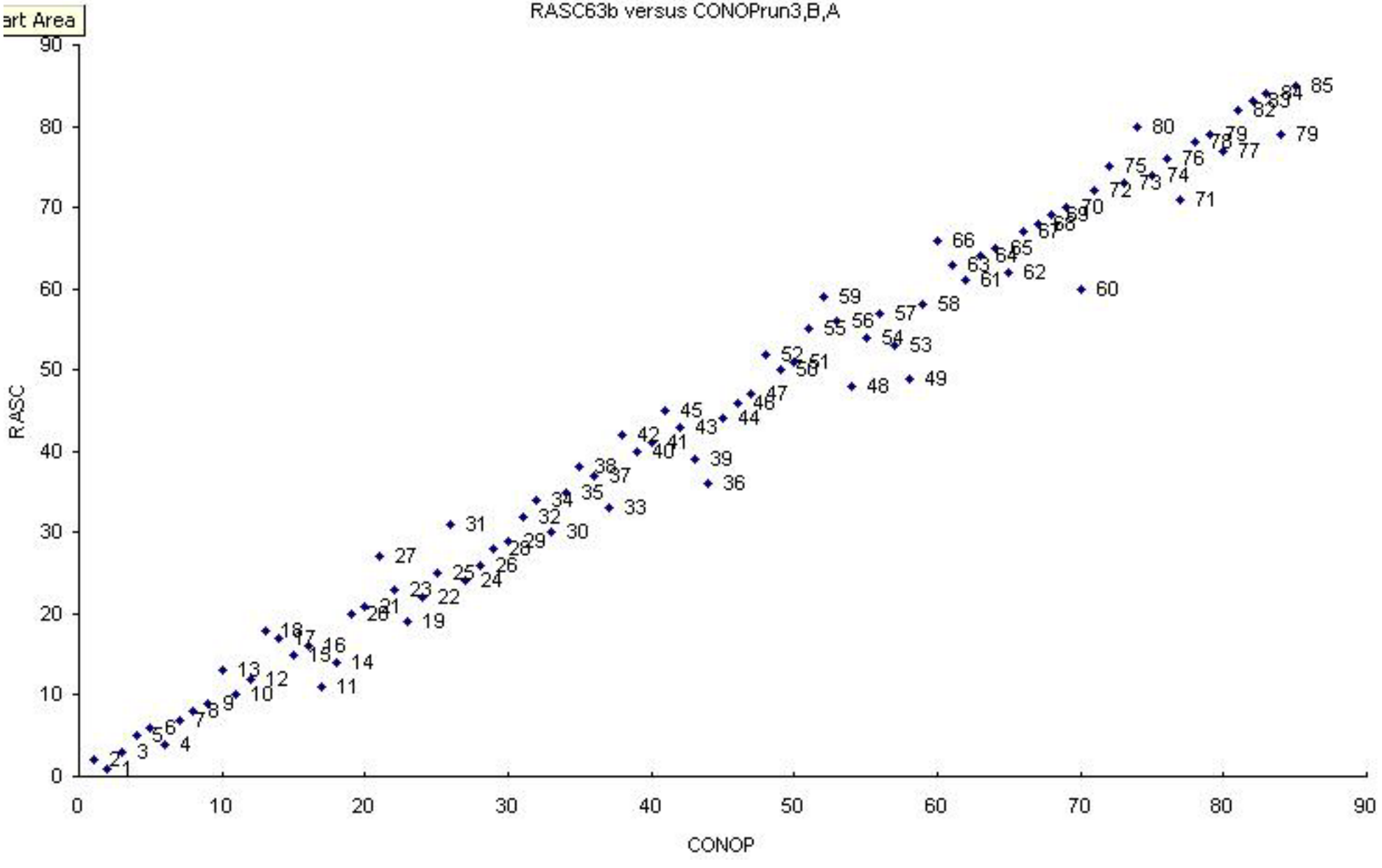
art Area
RASC63b versus CONOPrun3,B,A
RASC
CONOP
0
10
20
30
40
50
60
70
80
90

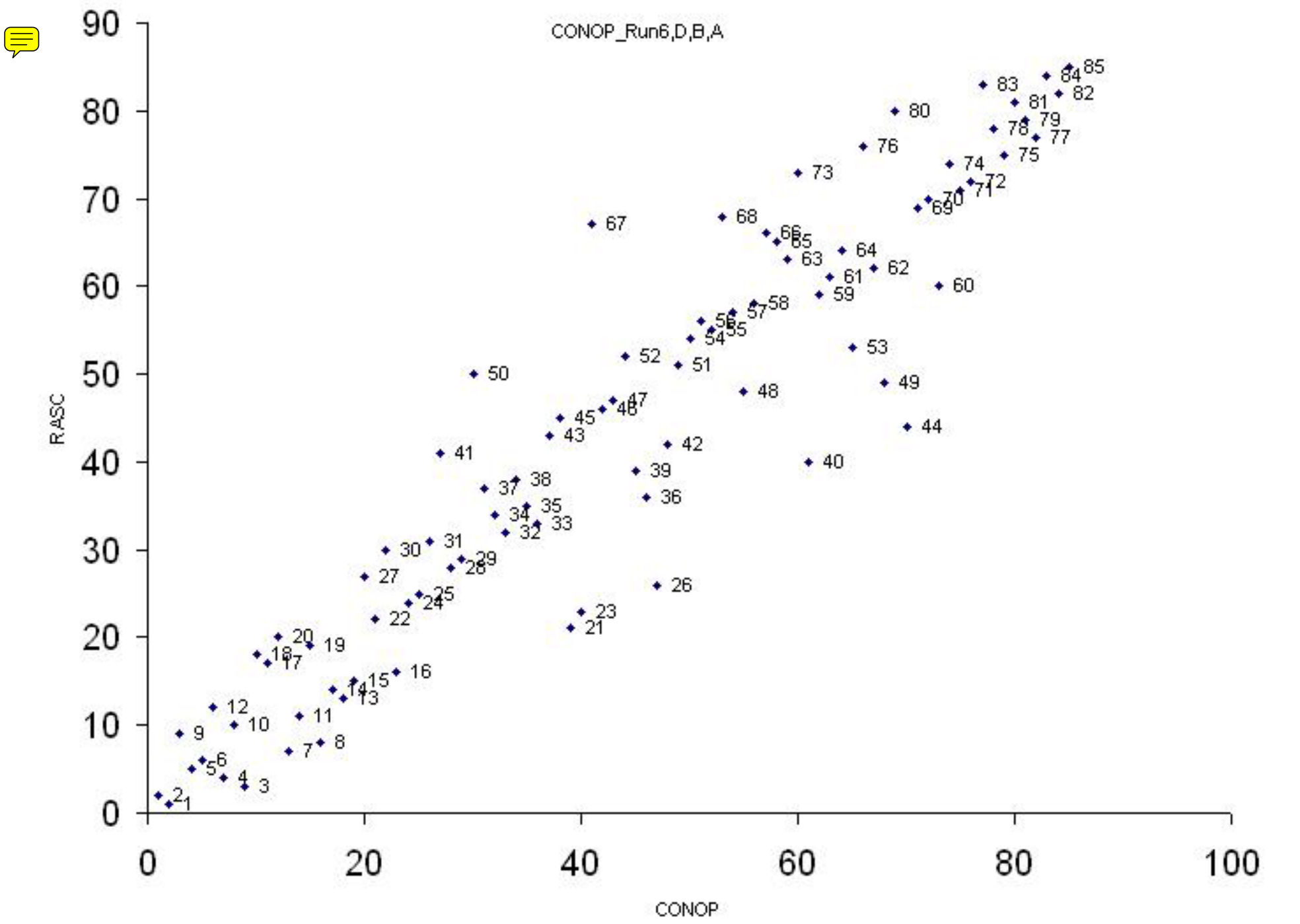
CONOP_Run6,D,B,A
RASC
CONOP
0
10
20
30
40
50
60
70
80
90
0
20
40
60
80
100

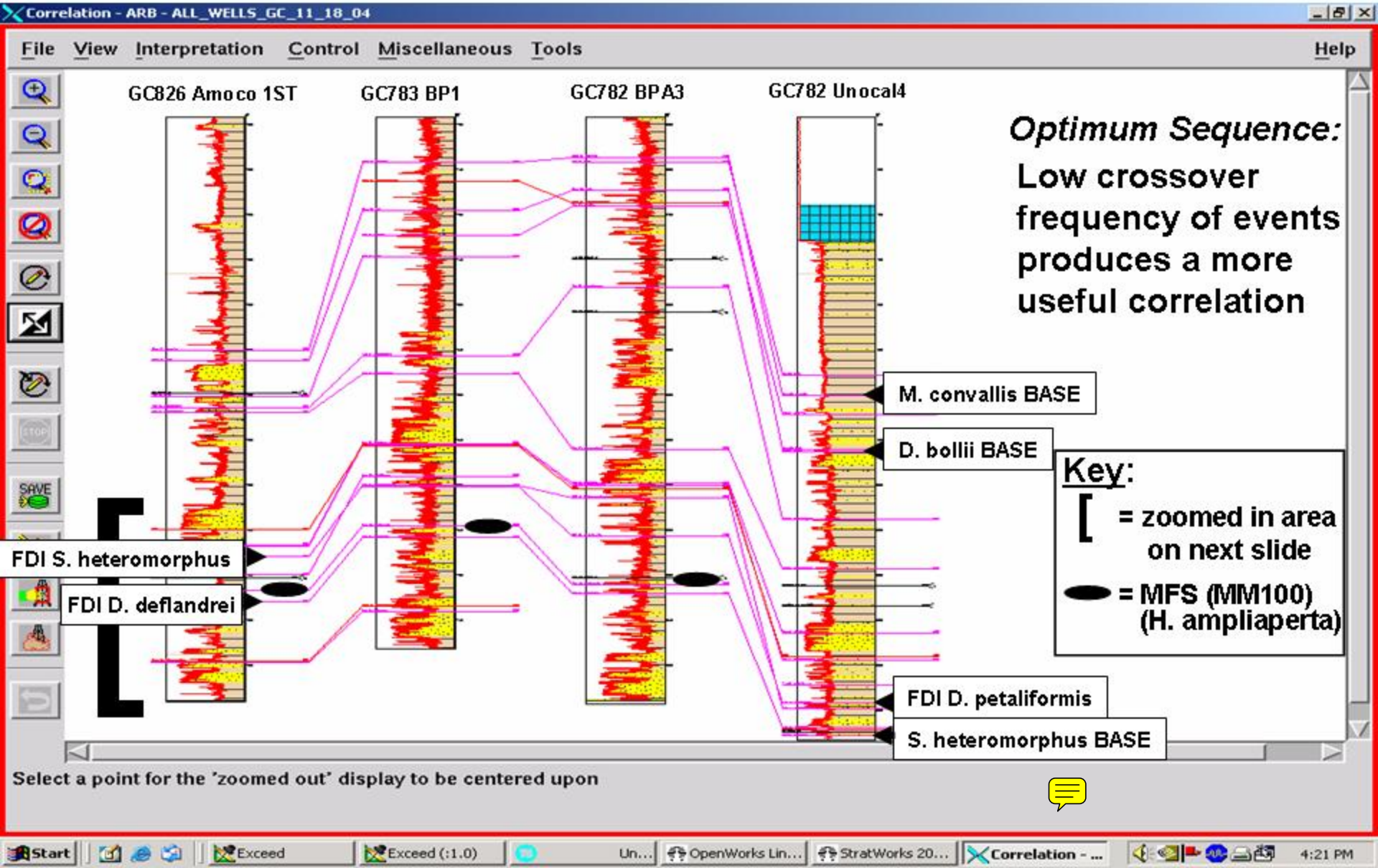
Correlation - ARB - ALL_WELLS_GC_11_18_04
File View Interpretation Control Miscellaneous Tools Help
GC826 Amoco 1ST
GC783 BP1
GC782 BPA3
GC782 Unocal4
Optimum Sequence:
Low crossover frequency of events produces a more useful correlation
M. convallis BASE
D. bollii BASE
Key:
= zoomed in area on next slide
= MFS (MM100) (H. ampliaperta)
FDI S. heteromorphus
FDI D. deflandrei
FDI D. petaliformis
S. heteromorphus BASE
Select a point for the 'zoomed out' display to be centered upon
Start
Exceed
Exceed (:1.0)
OpenWorks Lin...
StratWorks 20...
Correlation - ...
4:21 PM

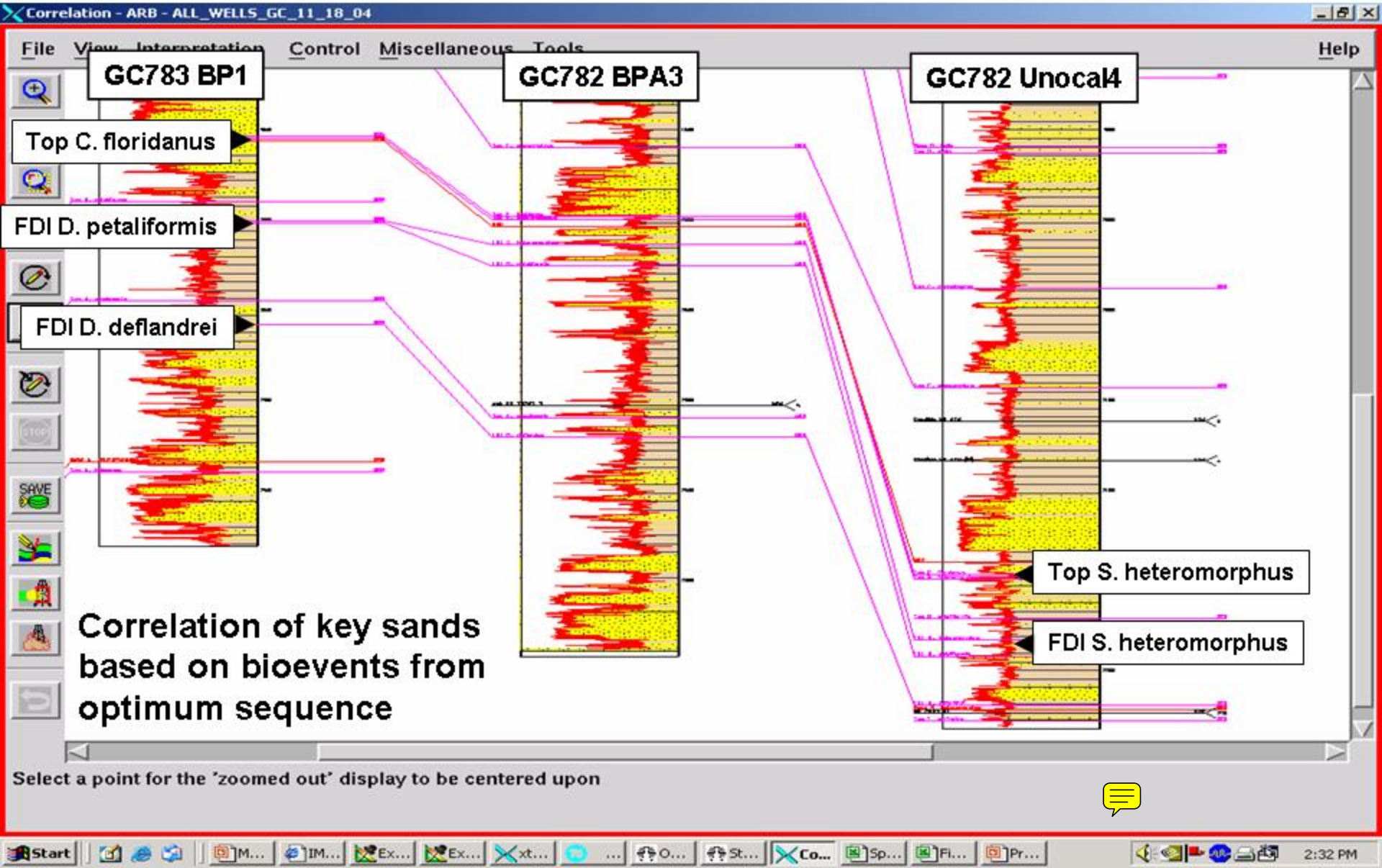
Correlation - ARB - ALL_WELLS_GC_11_18_04
File
View
Interpretation
Control
Miscellaneous
Tools
Help
GC783 BP1
GC782 BPA3
GC782 Unocal4
Top C. floridanus
FDI D. petaliformis
FDI D. deflandrei
Top S. heteromorphus
FDI S. heteromorphus
Correlation of key sands based on bioevents from optimum sequence
Select a point for the 'zoomed out' display to be centered upon
Start
2:32 PM